Visualization of Electromagnetic Field Intensities of Instrument Landing System

J. Honda
Researcher
Electronic Navigation Research Institute (ENRI)
Chofu, Tokyo, Japan
E-mail: j-honda@enri.go.jp

ABSTRACT

The Electronic Navigation Research Institute (ENRI) is a national research institute that supports the Japan Civil Aviation Bureau and airport authorities. The Instrument Landing System (ILS) is a highly reliable, traditional navigation system that precisely guides aircrafts approaching a runway. Japan is an isolated island nation wherein the area available for installing equipment is limited. Therefore, updating antenna systems and airports could result in significant changes in the ILS signal environment, leading to pilot report (PIREP) or monitoring errors of ILS ground system. Numerical simulations are commonly employed to understand and address these issues. Over the past decade, the ENRI has numerically evaluated the performance of ILS using the Geometrical Theory of Diffraction (GTD). However, since it employed computers with low specification, a simple algorithm was implemented and the signal environment was limited. To enhance the conventional simulation, we considered a new algorithm based on a hybrid numerical method. Additionally, a method for visualizing the propagation characteristics of electromagnetic waves generated by ILS is investigated that can be used by nonprofessionals to easily acquire the characteristics of the ILS signals. This paper presents procedures of our new numerical method and its numerical results.

INTRODUCTION

An Instrument Landing System (ILS) is a ground-based navigation aid that guides aircraft landings at airports [1]. It primarily comprises a localizer (LOC) and glide path (GP). The LOC provides horizontal guidance to ensure that an aircraft follows the appropriate approach course. The GP provides the vertical guidance of the appropriate path. The course/path is generated by synthesizing electromagnetic waves emitted from ground-based antenna systems. As shown in Fig. 1, the synthesized signals are amplitude modulated at 90 Hz and 150 Hz, and an aircraft determines its position based on the difference depth of the modulation (DDM) [2]. However, unexpected waves generated by obstacles and rough surfaces often penetrate the approach course/path and cause errors in the DDM, resulting in safety issues [1].

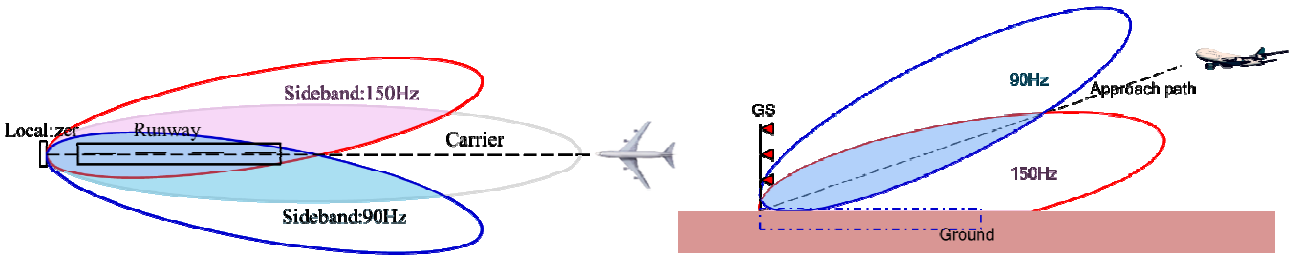

(a) Illustration of the LOC (b) Illustration of the GP

Fig.1 Overview of an ILS

Numerical simulations are crucial for addressing the operational issues in ILS and evaluating the electromagnetic interferences caused by obstacles and rough surfaces. Numerous studies on ILS have been conducted, and some simulators have also been developed [3]-[11]. ENRI conducted as well numerical simulations using the Geometrical Theory of Diffraction (GTD) to evaluate the performance of ILS in Japan for many years. Their accuracies were primarily validated through comparisons with experimental results. Although numerical simulations were useful, they had certain limitations. They could only tackle square-shaped two-dimensional (2D) obstacle and could not handle three-dimensional (3D) structures. Additionally, they only dealt with a single obstacle, and scattering from rough surfaces was out of target in the computation. Therefore, we received requests to update the numerical methods to handle more complicated signal environments. The ENRI investigated a new numerical method and considered the visualization of electromagnetic waves to enable users to easily understand the phenomenon of ILS signals. This paper introduces the overall concept of our new numerical method and presents visualized numerical results. First, a concept and procedures of a new algorithm based on the Ray-Tracing Method (RTM) are described. Subsequently, its numerical results are presented. The proposed numerical simulations visualize propagation path through obstacles and distribution of electromagnetic fields over the entire airport.

NUMERICAL METHOD

Related works

Numerical simulations are used to evaluate the interference of electromagnetic waves and assess the ILS performance. In related studies, numerical simulations have been conducted using physical optics (PO), finite difference time domain (FDTD), method of the moment (MoM) and high-frequency method based on geometrical theory of diffraction (GTD)/ uniform geometrical theory of diffraction (UTD) [4],[5],[7],[8],[9]. The MoM obtains the most accurate results; however, it is computationally expensive and difficult to implement on regular computers. By contrast, the PO and the GTD/UTD can be easily employed in simulations, and their performances have been validated in various studies. The ENRI employed GTD in the previous simulation.

Numerical method

The proposed numerical method is based on the RTM, which is classified as a high-frequency method. A standard computational procedure of RTM is as follows: first is to search rays from a source to a receiver, and second is to compute electromagnetic fields based on the ray data. A computational procedure of our computation based on the RTM is illustrated in Fig. 2, which begins with the preparation of an airport layout and obstacles, such as terminal buildings, are generated using polygon facets. A representative point at any location on the facet is then determined. The RTM clarifies the positional relationship using these representative points to determine whether the transmitter, receiver, and obstacles are in line-of-sight (LOS). A propagation path from a transmitter to a receiver is created by connecting the representative points when they are in LOS [2]. This approximate ray can be modified into an accurate ray using the imaging method. This simple implementation requires minimal computational memory and time. Next, we proceed to the field computations. A hybrid numerical simulation is employed to select the appropriate numerical methods by judging the obstacle size. The general high-frequency method is employed if the obstacle size is larger than the several wavelengths; otherwise, full-wave analysis is employed. Fig. 2 presents a flowchart of the proposed algorithm that is still under development. However, a part of its high-frequency implementation has been completed.

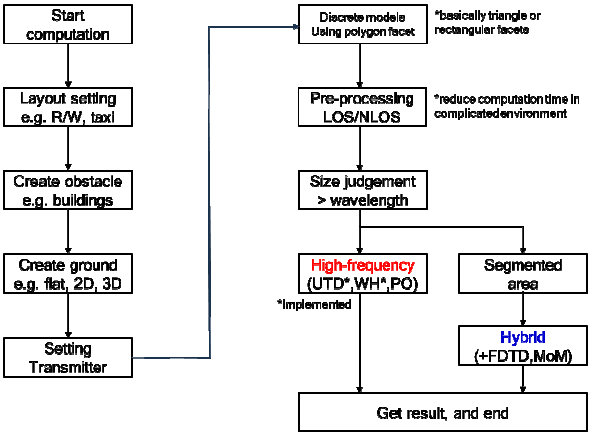

Fig.2 Flowchart of the proposed algorithm

The GTD and UTD are typically used to compute the scattered fields from obstacles. In this study, scattered waves are computed using an approximation based on the Winner-Hopf (WH) solution, whose accuracy is similar to that of the UTD. The accuracy was verified by comparing the results with those of circular scattering [12]. Diffraction can be classified as source (incident) diffraction or reflected diffraction. When the reflected field dominates in the total field, including reflected diffraction could be sufficient for the total field.

The imaging method of the RTM is also employed. A single reflected wave is generated by the facet of an obstacle, and a combination of waves diffracted by the edges of the facet is computed as shown in Fig. 3 [2]. Therefore, the total field from a single facet is the sum of the single reflection and diffractions caused by the edges. However, the diffractions from the edges in contact with the ground and multiple diffractions are ignored.

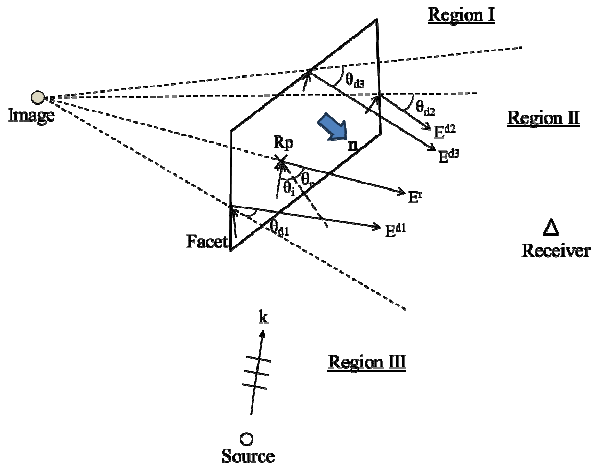

Fig.3 Classification of scattered waves.

The total field differs depending on the order of scattering because the RTM has many rays corresponding to the times of reflection and diffraction. The scattering order can be classified as follows:

- Zeroth-order scattering: incident wave (i)
- First-order scattering: ground reflection (gr), reflected waves (r), and diffracted waves (d)
- Second-order scattering : two-times reflection (r2) and diffraction (d2), reflection-diffraction (rd), and diffraction-reflection (dr).

Second-order scattering includes both obstacles and ground reflections. However, for simplicity, we neglect multiple reflections/diffractions from the obstacles. Different total fields corresponding to the scattering order are prominent in analog

systems such as the ILS. Therefore, the appropriate scattering order should be selected based on the propagation environment when RTM is employed.

Numerical simulation outputs

Table 1 lists the outputs of the proposed numerical method.

Table 1. Outputs of the proposed numerical method

Class	Contents
Antenna/Transmitter	Radiation from the antenna element
	Ideal radiation from LOC/GP - Three types of LOC transmitter are used in Japan: single frequency with 14 LPDAs (1f14LOC), single frequency with 24 LPDAs (1f24LOC), dual frequency with 24 LPDAs (2f24LOC)
Propagation path	Rays: incident, reflected, diffracted, and their combinations *
Fields	Electric field at a single point
	Electric fields along the flight path
	Electric field distribution on the airport layout *
DDM	DDMs along the flight path
	DDM distribution on the airport layout *

* Illustrations for the visualization of ILS signals.

NUMERICAL RESULTS

Based on outputs of the proposed numerical method listed in Table 1, this section presents some numerical results. Fig. 4 illustrates a sample airport layout that includes 30 obstacles of various shapes. The runway is 3000 m long, and the LOC is placed at 300 m from the end of the runway, and the GP is placed approximately 315 m from the end of the runway and 120 m from the runway center line.

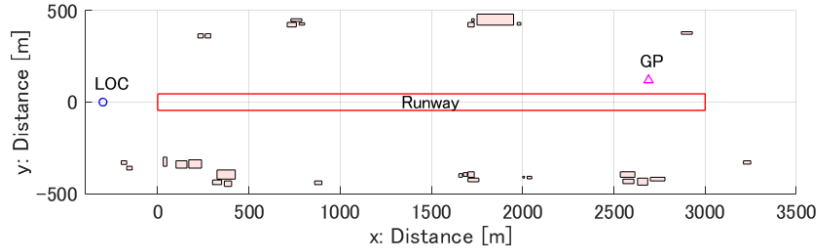

(a) 2D view

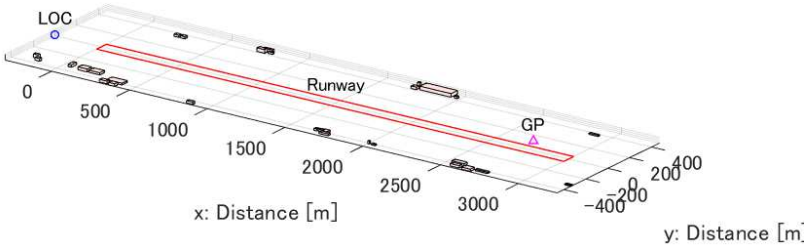

(b) 3D view

Fig.4 Sample airport layout.

Fig. 5 shows the radiation patterns of the LOC and GP, respectively. The LOC radiation is based on the 1f24LOC and its GP comprises an M-array. The values are obtained at a distance of 10 NM from the transmitter. Fig.5(a) shows the LOC radiation patterns, where the carrier and sideband waves are illustrated by blue and orange lines, respectively, and the vertical axis represents the electric power in dBuV/m. Fig.5(b) shows the GP radiation patterns where the carrier, sideband and clearance waves are illustrated by blue, orange and yellow lines, respectively, and the vertical axis represents electric fields in uV/m.

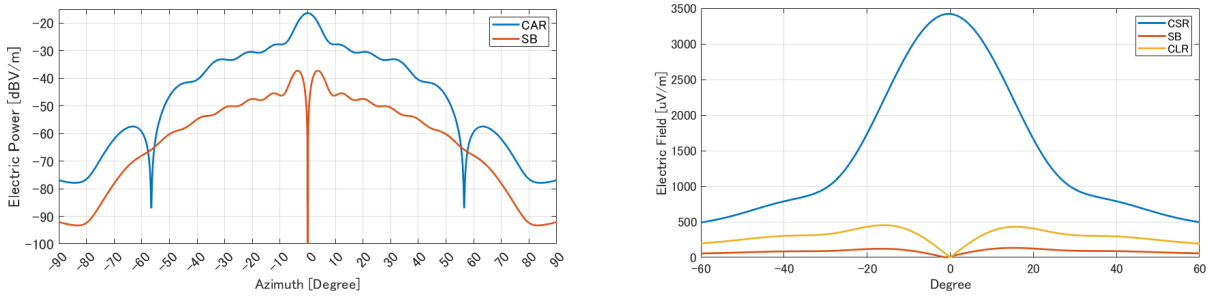

(a) LOC (b) GP

Fig.5 Radiation pattern.

Fig. 6 shows the ray distributions with up to first and second order of scattering. The receiver is located at 1400 m at a height of 4.0 m above flat ground. Each ray component has a different color. Rays are emitted from 24 LPDAs, diffracted rays occur at edges of each facet in the LOS situation, and the reflected rays arrive at the receiver through an obstacle at the lower left. The ray distribution indicates the location from which the ILS signal arrives at the receiver. All rays are used for computing electric fields when UTD/GTD/WH is selected. In contrast, the rays are used to determine the LOS/NLOS situation to compute the electric current on each facet when the PO is selected. The ray computation process for the GP is basically similar to that of the LOC.

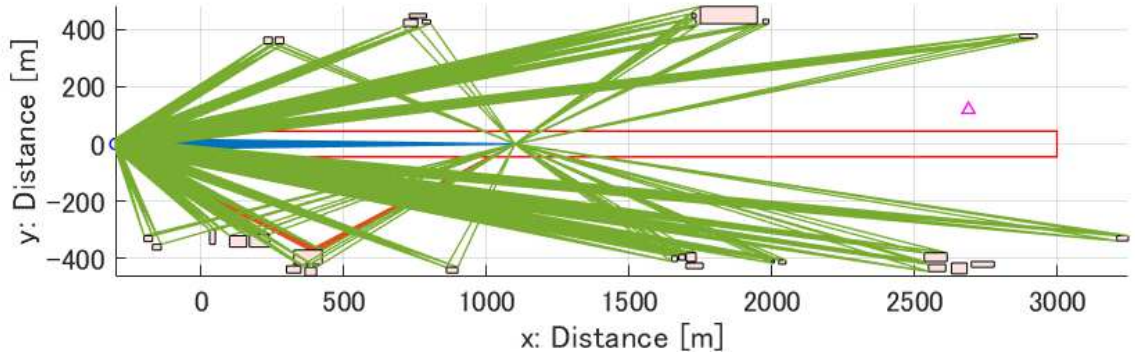

(a) Rays up to the first order scattering

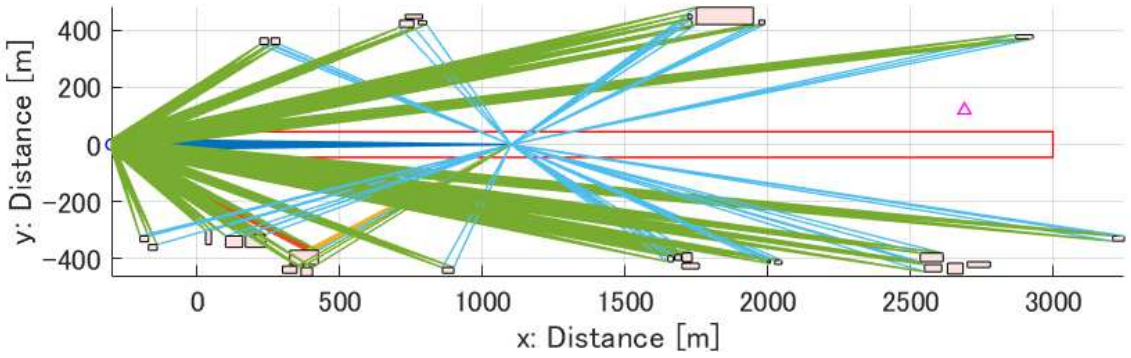

(b) Rays up to the second order scattering

Fig.6 Propagation paths from LOC.

Fig. 7 shows the electric field distributions for the LOC and GP. Axis indicates distance in m expression, the runway is shown by red solid line, and obstacles are illustrated in blue square. Field intensities are expressed in color gradation whose unit is in dB. Fig. 7(a) shows the field distribution of the LOC, where the top panel shows the carrier wave and the bottom panel shows the sideband wave. The location where the scattered waves penetrate the centerline of the runway is clear visible. Fig. 7(b) represents the field distribution of the GP; the top panel shows the carrier wave, the middle panel shows the sideband wave, and the bottom panel shows the clearance wave. All signals are influenced by the scattered fields caused by the obstacles.

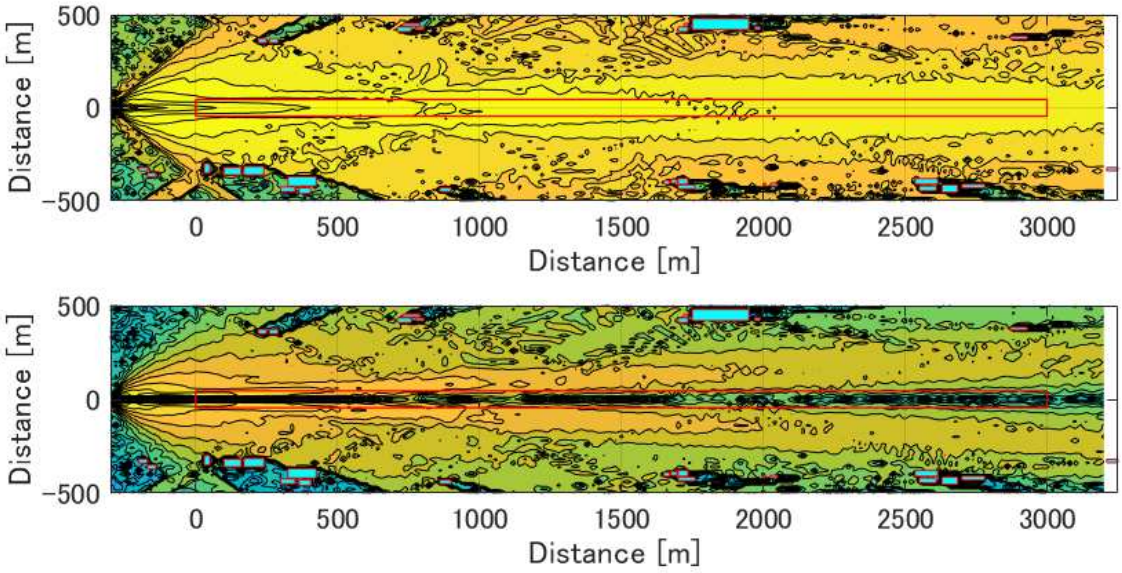

(a) LOC signal distribution (top: carrier; bottom: sideband)

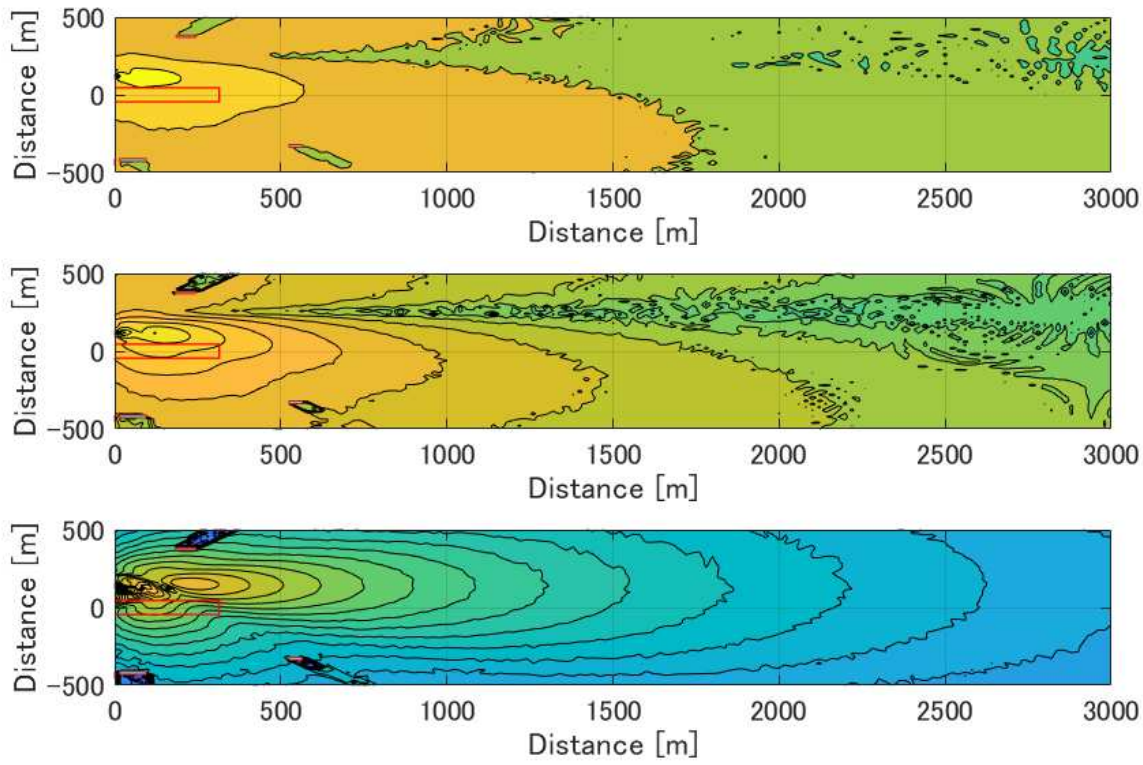

(b) GP signal distribution (top: carrier; mid: sideband; bottom: clearance)

Fig.7 Electric field distribution of the LOC and GP.

Fig. 8 shows the DDM distributions for the LOC and GP. The color gradation is expressed in uA in the range between ±300. The fluctuations in the DDM and its strength are illustrated. They mention the location where the influences from obstacles appear. Visualizations are useful for acquiring the signal environment in the vicinity of the airport. As mentioned at the beginning of this paper, many numerical simulations have been conducted and validated. However, visualization is another effective approach for understanding the characteristics of ILS signals. Such this visual expression can also be applied to other wireless systems.

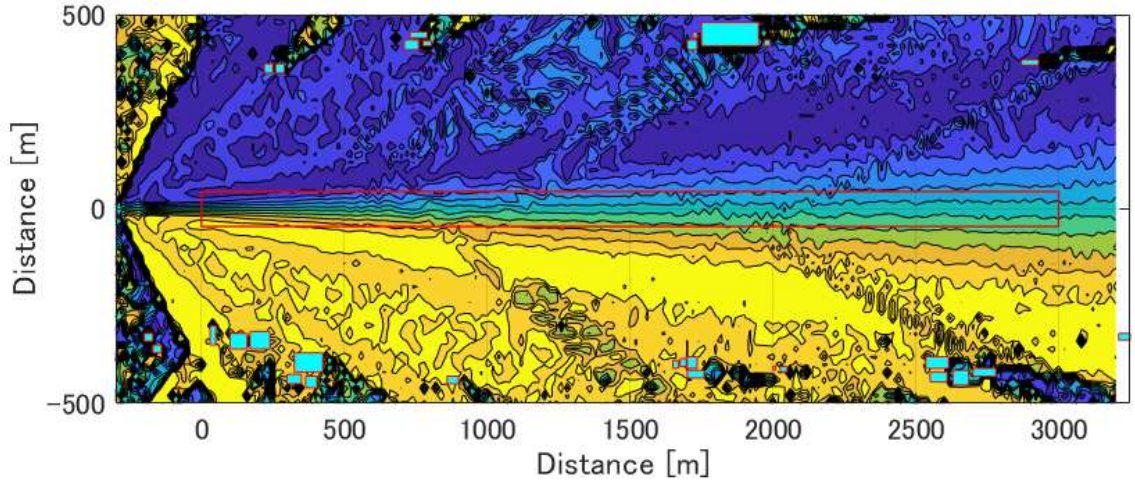

(a) LOC

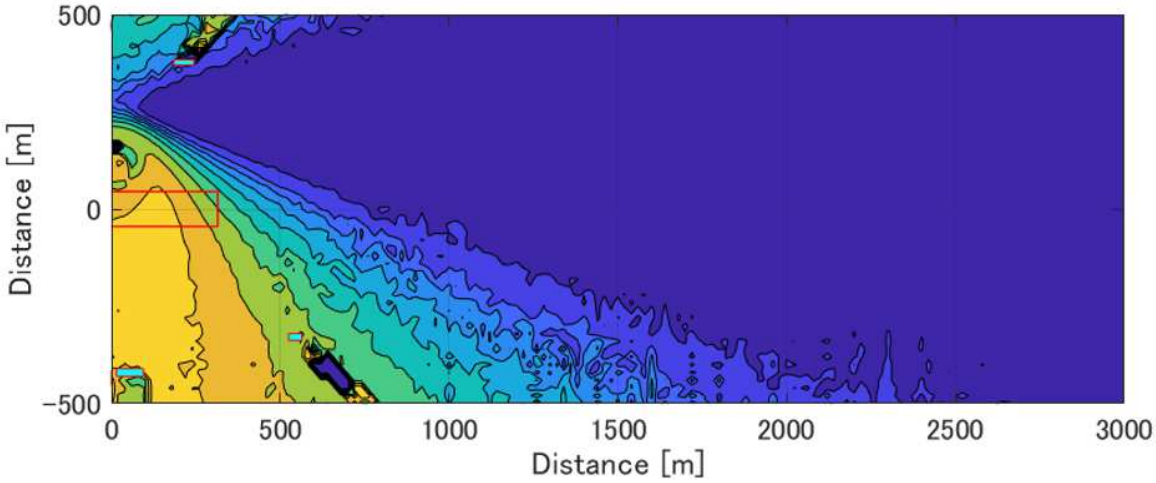

(b) GP

Fig.8 DDM distribution.

CONCLUSIONS

This paper discussed the ILS signals from a numerical perspective and proposed a new numerical method for understanding and visualizing the ILS signal characteristics, which is a significant improvement over our previous numerical simulations. The proposed numerical method was based on the hybrid method; however, it is still under development. A high-frequency based numerical simulation was conducted in this paper, and an approach based on the visualization of ILS signals was then employed. Numerical results demonstrated the origin of the scattered waves as well as their penetration locations on the landing course/path.

FUTURE WORK

This paper reported the initial developments of a new numerical method for visualizing ILS signals; however, further modifications are required to complete this hybrid method. This will be the focus of our future work.

REFERENCES

[1] Aeronautical Telecommunications Annex 10 Volume I Radio Navigation Aids, 6th edition, ICAO (International Civil Aviation Organization), QC Canada, 2006.

[2] J. Honda, “Influence of Scattering Order on ILS Localizer Using Ray-Tracing Method,” Proc. Int. Symp. on Antennas and Propagation (ISAP), 1570923000, pp.1-2, Kuala Lumpur, Oct.-Nov. 2023.

[3] R.W. Redlich and J.T. Gorman, “Disturbance of ILS Localizer Signals by Reflections from Large Hangers,” IEEE Trans. Aerospace and Electronic Sys., Vol.AES-5, pp.1001-1002, Nov. 1969.

[4] S. L. Shin, “ILS Localizer Multipath Analysis,” IEEE Trans. Aerospace and Electronic Sys., Vol.AES-7, No.1, pp.54-60, Jan. 1971.

[5] A. Thain, J-P. Estienne, J. Robert, G. Peres, G. Cambon, L. Evain, B. Splitz, “A Solution for ILS Disturbance Due to a Building,” Proc. the 6th European Conference on Antenna and Propagation (EuCAP), pp.2392-2395, March 2012.

[6] A. Thain, J.P. Estienne, G. Peres, B. Spitz, L. Evain and M. Kumar, “Comparisons of Different Approaches for ILS Simulation,” Proc. the 4th European Conference on Antenna and Propagation (EuCAP), pp.1-5, Barcelona, Spain, April 2010.

[7] R. Geise, J. Schueuer, L. Thiele, K. Notte, T. Beckers and A. Enders, "A Slotted Waveguide Setup as Scaled Instrument-Landing-System for Measuring Scattering of an A380 and Large Objects," Proc. the Fourth European Conf. Ant. and Propag. (EuCAP 2010), pp.227-231, Barcelona, Spain, April 2010.

[8] G. Greving and W.D. Biermann, "Theoretical Aspect and Numerical Solution of Scattered from Objects under Grazing Angle Incidence - The A380 and the Aircraft Tailfin," Proc. the 37th European Microwave Conf., pp.1369-1372, Munich, Germany, Oct. 2007.

[9] J. Godfrey et al., "Terrain modeling using the half-plane geometry with applications to ILS glide slope antenna," IEEE Trans. Antennas and Propagation, Vol.24, pp.370-378, May 1976.

[10] R. Luebbers, V. Ungvichian and L. Mitchell, "GTD Terrain Reflection Model Applied to ILS Glide Scope," IEEE Trans. Aerospace and Electron. Sys., Vol.AES-18, pp.11-20, Jan. 1982.

[11] E.K. Walton, "Effect of wet snow on the null-reference ILS system," IEEE Trans. Aerospace and Electron. Sys., Vol.29, pp.1030-1035, July 1993.

[12] K. Uchida, J. Honda, and K. Y. Yoon, "Approximate Solution to Wedge Diffraction for Discrete Ray Tracing Method," Proc. KJJC-AP.EMC/EMT 2009, pp.303-306, Korea, May 2009.